DP-MS-83-62

DEVITRIFICATION BEHAVIOR OF SRL DEFENSE WASTE GLASS

by

Dennis F. Bickford and Carol M. Jantzen

E. I. du Pont de Nemours & Co.
Savannah River Laboratory
Aiken, South Carolina 29808

A paper for presentation and publication in the proceedings
Materials Research Society Annual Meeting
Boston, MA
November 14-17, 1983

DEVITRIFICATION BEHAVIOR OF SRL DEFENSE WASTE GLASS

Dennis F. Bickford and Carol M. Jantzen
E. I. du Pont de Nemours & Co., Savannah River Laboratory
Aiken, South Carolina 29808

ABSTRACT

Simulated SRL waste was prepared with compositions varying in iron and aluminum content. Two batches with similar composition were produced with different amounts of reducing agent added. Samples were isothermally heat treated and used to derive time-temperature-transformation diagrams. Supplementary samples were cooled in a manner programmed to simulate the cooling curves of production canisters. Less than 10% total devitrification occurs during normal processing. However, when waste glass 165 was purposely devitrified, up to 30 volume percent total spinel and acmite formed. Formation of these species had minor effect on leachability in MCC-1 and accelerated leach tests.

INTRODUCTION

Nuclear waste glasses can transform into more ordered crystalline phases at temperatures below the liquidus. Crystallization, or devitrification, of waste glasses can occur during slow initial cooling of the melt, during subsquent processing, or during storage at elevated temperatures. Determination of the crystallization kinetics from experimental time-temperature-transformation (TTT) diagrams allows the effects of certain accident scenarios which result in elevated temperatures to be assessed, e.g., transportation fires. They also are indicative of the relative stability of glasses to long time, moderate temperature behavior, e.g. 10^6 to 10^8 years in repository storage [1].

Devitrification may be considered advantageous or deleterious depending upon the particular formulation, and the devitrification's effect on mechanical, thermal, or chemical stability. Crystals may also modify the properties of the vitreous matrix by shifting the balance between network formers, modifiers, and intermediates.

The first detailed studies of devitrification of waste glasses demonstrated that although the waste-glass systems are complex, the kinetics follow trends based on theoretical models of simple glasses [2,3]. Kinetically, a free energy barrier stabilizes the vitreous state, and growth of any nuclei is limited by diffusion. Hence, a "nose" exists in the TTT curve which represents the minimum time required for a given volume fraction to crystallize. This results from a competition between the driving force for crystallization, which increases with decreasing temperature, and the molecular mobility, which decreases with decreasing temperature [4]. In the nucleation and growth process, the principal limit to the establishment of the new phase is an interface, (either chemical, structural, or both), unless melt-nucleating heterogeneities, e.g., melt insolubles, are present.

The information contained in this article was developed during the course of work under Contract No. DE-AC09-76SR00001 with the U.S. Department of Energy.

The effects of melt insolubles and oxygen fugacity on devitrification kinetics have been examined for SRL waste glass formulations with average defense waste sludge [5]. In this study, the behavior of a similar formulation incorporating defense waste sludge with a higher aluminum content is added, and compared to the average composition. TTT diagrams, kinetics of devitrification, and the relative leachability of waste glass as a function of devitrified phase development are discussed.

EXPERIMENTAL PROCEDURE

Simulated waste sludge batches were prepared from reagents and premelted glass frit [5]. Compositions are shown in Table I. Formic acid was refluxed with sludge prior to frit addition. The formic acid reduces the valance of transition metals. Samples with reduced oxygen fugacity were melted and heat treated in closed crucibles. Mossbauer spectroscopy indicates a Fe^{++}/Fe^{+++} ratio for 165 UTDS of 0.27 $\pm$ .02 at a 95% confidence level. This corresponds to an oxygen fugacity of 10^{-6} atmospheres at 1150°C [6]. Batch 165U was melted in air, and had a Fe^{++}/Fe^{+++} ratio of 0.00 $\pm$ 0.01, indicating complete oxidation and

TABLE I. Chemical Composition of Melt Simulations

Chemical	165 Average Composition Melter Feed, wt %	165 High Aluminum Composition, wt %	Chemical	165 Average Composition Melter Feed, wt %	165 High Aluminum Composition, wt %
SiO_2*	42.648	42.247	Ag	0.029	0.000
B_2O_3*	6.272	6.213	Cu_2O	0.031	0.024
Na_2O*	8.153	8.077	$CoCl_2 \cdot 6H_2O$	0.004	0.000
Li_2O*	4.390	4.349	Zn	0.062	0.021
MgO*	0.627	0.621	$Mg(NO_3) \cdot 6H_2O$	0.668	0.781
ZrO_2*	0.627	0.621	$Na_3PO_4 \cdot 12H_2O$	0.020	0.052
Fe_2O_3	9.234	5.013	NaF	0.030	0.157
$Mn(COOH)_2$	4.594	2.866	Cs_2O	0.028	0.028
$UO_2(NO_3)_2 \cdot 6H_2O$	3.370	1.362	Coal	0.023	0.000
$Al(OH)_3$	5.804	11.051	Zeolite†	2.108	0.000
$CaCO_3$	1.281	1.171	Na_2SO_4	0.055	0.254
$CaSO_4$	0.064	0.000	KOH	0.093	0.084
PO_4	0.035	0.036	$Sr(NO_3)_2$	0.065	0.060
CaF_2	0.030	0.000	HCOOH (90%)	4.03††	0.000††
NiO	0.747	0.538			
NaCl	0.102	0.000	SiO_2	0.883¶	0.755¶
HgO	0.673**	0.667**	Al_2O_3	0.040¶	0.971¶
NaI	0.003	0.000	B_2O_3	0.090¶	0.089¶
RuO_2	0.090	0.090¶¶	Alkali	0.560¶	0.614¶
$Na_2SiO_3 \cdot 9H_2O$	6.735	14.601	Alkali earth	0.035¶	0.031¶
ThO_2	0.237	0.867	Fe	0.087¶	0.063¶
BaO_2	0.085	0.062	Other transition metals	0.073¶	0.034¶
$Ce(SO_4)_2$	0.237	0.063	Rare earths	0.001¶	0.000¶
$PbSO_4$	0.129	0.008	U, Th	0.008¶	0.006¶
La_2O_3	0.182	0.099			
ZrO_2	0.166	0.146			
$CrCl_3 \cdot 6H_2O$	0.408	0.390			

* Added as -80 mesh frit
** Not added to simulation
† Linde AW500
†† Composition expressed as cc/100 g
¶ Composition expressed as mol/100 g
¶¶ Equivalent added as soluble chloride

equilibration with air. Specially prepared x-ray diffraction and magnetic susceptibility standards were utilized to determine the extent of devitrification [7].

Ceramographic samples were prepared from annealed glasses by using standard methods. After carbon coating, they were examined by SEM-XES at 30-2500X for qualitative characterization of the devitrified phases. Spectra were assessed both by counting and by digitally subtracting the signal of particles from the signal of the surrounding material. Electron beam microprobe analyses were used for quantitative phase determination.

Leach studies used an analytical method developed by Corning Glass Works (CGW). Samples for comparative leach studies were ground and sieved to between 100 and 200 mesh, giving an estimated average spherical particle size of 1.11×10^{-2} cm. In this test, 2 g of crushed sample was placed in 100 mL of deionized water in a polyethylene bottle. The bottle was placed in an 80°C convection oven for 24 hours and then removed and allowed to cool. The pH was measured and an aliquot of the leachate was analyzed by inductively coupled plasma (ICP) for B, Si, and Na. Additional monolithic samples were leached by the MCC-1 static leaching procedure [8] at 90°C.

KINETICS

The TTT diagrams for SRL 165-Stage I waste glass determined by combined x-ray diffraction analysis and magnetic susceptibility measurements are shown in Figure 1. The TTT diagram for average composition samples prepared and annealed in air (165U) has two distinct regions, glass + spinel and glass + spinel + acmite. In the glass + spinel + acmite region, the fraction of spinel crystallized appears to decrease as the volume fraction of acmite increases at a given temperature. In the glass prepared and annealed under reduced fO_2, the crystallization of spinel and acmite are separate. X-ray diffraction did not indicate the presence of spinel in high aluminum glass (Figure 1) but a small amount (less than 1 volume percent) of spinel was found by optical microscopy and SEM in the 900°C and 800°C isothermal anneals.

Continuous cooling curves measured at reference pour rates at the surface and centerline of 24-inch diameter canisters are also shown in Figure 1. Samples that were program cooled behaved in a manner consistent with the rules for applying isothermal TTT diagrams to continuous cooling [9].

The data for the reduced average glass composition (Figure 1A) suggests that crystallization occurs in the 600 to 700°C regime more rapidly than for more oxidized glasses (Figure 1B). The influence of iron on the rate of crystallization in silicate and phosphate based radioactive waste glasses shows similar trends [10]. The incubation times for the crystallization of reduced glass are smaller, but the total percentage of crystallinity, especially the total percentage of acmite, is lower than for the oxidized glass. Similar trends are found for spinel and acmite crystallization in basalt glass-ceramics formed under oxidizing and reducing conditions [11].

The percent total crystallinity was used to develop [2,3] Arrhenius plots. An activation energy for devitrification of the oxidized composite glass is approximately 17.7 kcal/mol and represents the total process of spinel nucleation plus consumption of spinel during the growth of acmite.

165UTDS: AVERAGE COMPOSITION GLASS

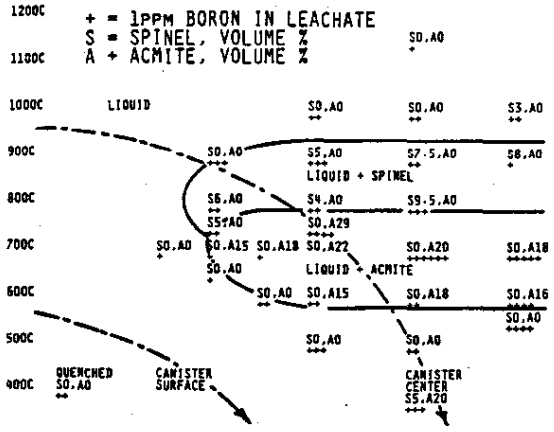

SRL 165U: OXIDIZED AVERAGE COMPOSITION

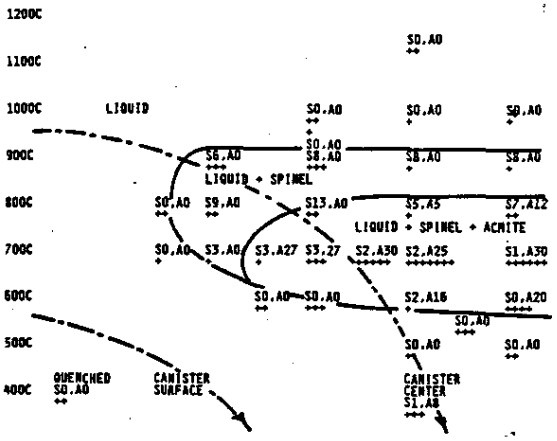

SRL 165HiAl: HIGH ALUMINUM GLASS

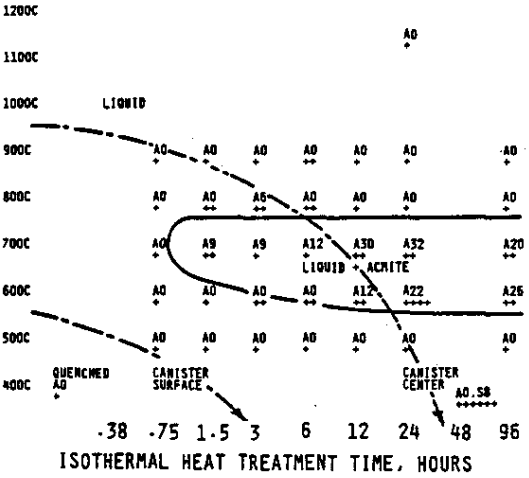

FIG. 1. Experimentally determined TTT diagrams for SRL waste glasses. Full scale operations result in a family of cooling curves lying between the canister surface and canister centerline cooling curves.

The nominal $NaFeSi_2O_6$ contained 7.1 atomic percent Fe in 165UTDS, and 4.4 atomic percent Fe in 165HiAl, approximately proportional to its decrease in the bulk. Similar small shifts occurred in Mn and Ni content, and the aluminum increased from 0.39 atomic percent in the acmite in 165UTDS to 1.05 in 165HiAl. A major portion of the alkali is believed to be Li, which cannot be analyzed by SEM or electron microprobe. The crystal morphology of the acmite in 165HiAl is more idiomorphic with an increased tendency to form facets, implying a higher surface free energy [12]. Thus, the lower crystallization rate is probably the result of the increased surface free energy.

MICROSTRUCTURE

Heterogeneous nucleation was observed to occur on individual and clustered RuO_2 particles. During 800 to 900°C heat treatments of average composition melted in air, spinel nucleated and grew with an average composition of $(Ni_{0.85}Mn_{0.15})(Fe_{0.8}Cr_{0.2})_2O_4$ (Figure 2A). Growth of spinel was most rapid at 900°C. At 800 to 900°C under reduced oxygen fugacity, the Fe^{3+} replaced most of the Cr^{3+}, and Ni^{2+} replaced almost all of Mn^{2+}. The resulting average spinel composition was $(Ni_{0.95}Mn_{0.05})(Fe_{0.95}Cr_{0.08})_2O_4$. This spinel was slower to grow, perhaps because it required the diffusion of Fe^{2+} away from the interface, whereas the oxidized glass was Fe^{2+} free.

Between 800 and 550°C, an acicular nickel-rich iron silicate was heterogeneously nucleated on RuO_2 (Figure 2B). The approximate atomic composition was 4% Na, 2% Mn, 2% Al, 5% Ni, 7% Fe, 18% Si, and 60% O_2, suggesting a substituted $NaFeSi_2O_6$. This acted as a host nucleus for massive acmite formation (Figure 2C). Acmite compositions were depleted in Fe and enriched in Si for the oxidized samples. At 550°C and below, growth was prevented, presumably by low atomic mobility.

In the high aluminum glass, a small amount of $Ni(Fe_{0.5}Cr_{0.5})_2O_4$ formed at 800 and 900°C, but stopped growing once the chromium was depleted in the matrix. The increased concentrations of nickel and chromium relative to the feed composition are an indication that the high free-energy form $NiCr_2O_4$ is favored over the lower free-energy spinels, e.g., $MnFe_2O_4$ or Fe_3O_4. Optical and SEM examination did not indicate any fracture of the glass matrix caused by differential thermal expansion of devitrified phases.

To examine the effect of melt insolubles such as RuO_2, and possibly Cr, on heterogeneous nucleation, two series of experiments with a simpler glass formulation were examined. The samples were doped with RuO_2 and/or carbon to vary melt insoluble and oxygen fugacity simultaneously. In the first series of tests the absence of RuO_2 and Cr suppressed measurable nucleation and growth for 96 hours at 600°C. The second series of tests confirmed that the amounts of RuO_2 and reducing agent are important for nucleation and growth of secondary phases. The most extensive devitrification occurred when the RuO_2 was present in reduced glass. Similar nucleating effects of RuO_2 in waste glasses have been previously reported [13,14]. RuO_2 appears to be an effective nucleating agent for waste glass because of its low solubility [2,3,15], high melting point, and high specific area.

LEACHING BEHAVIOR

A 24-hour leach test of powdered devitrified glass was used for the determination of differential leaching as a function of phase development. Values of pH, Si, Na, and B were contoured on the TTT diagrams but consistent trends were only observed for the release of

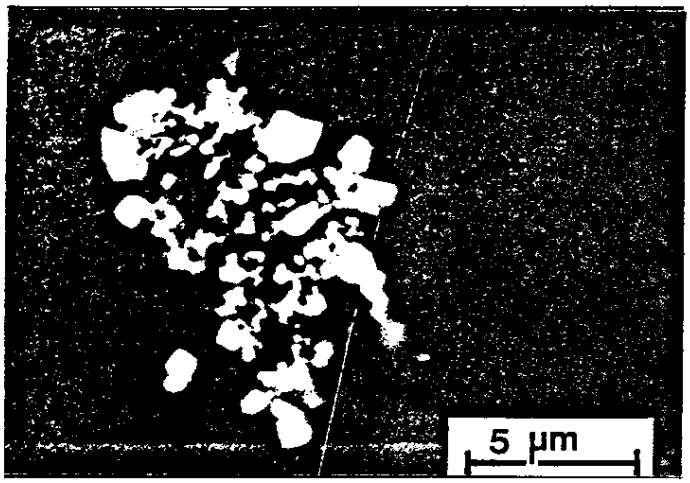

A. Spinel growing on RuO_2 cluster (165U glass heat treated at 800°C for 24 hours)

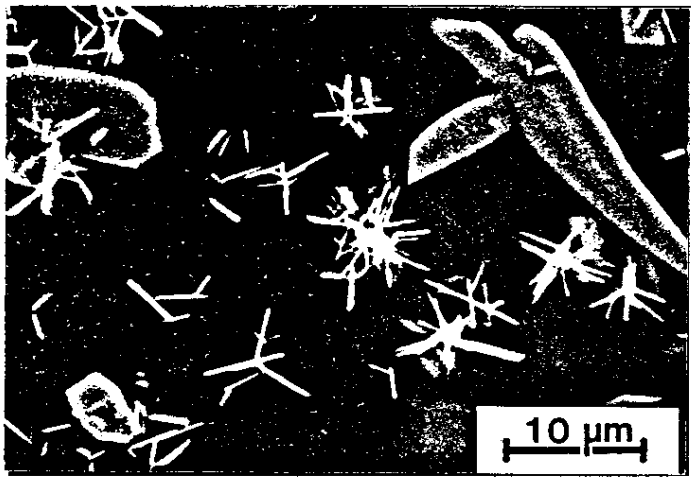

B. Acicular acmite growing on RuO_2 particles and massive acmite growing acicular acmite (165U glass heat treated at 700°C for 3 hours)

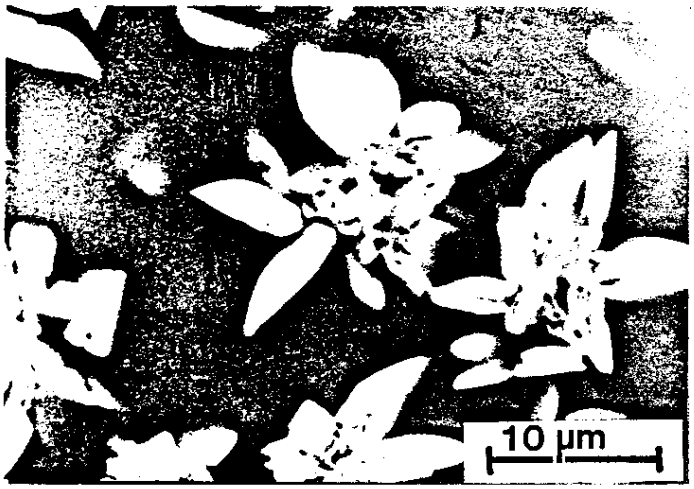

C. Massive acmite growing on RuO_2 particles (165U TDS glass heat treated at 700°C for 24 hours)

FIG. 2. Photomicrographs of devitrification products. Note role of RuO_2 as a nucleating agent.

the glass matrix element boron (Figure 3). The poor correlation of phase development with Si and Na may be due to their dual role in both the glass matrix and in the crystallization of acmite. The poor correlation with pH was due to the small range of values observed.

In the region of the TTT curve where acmite crystallizes (Figures 1 and 3) boron release increases by a factor of about three. In the region of spinel devitrification, the release of boron is virtually the same as in regions of no crystallization. In the high aluminum waste, the ingrowth of acmite resulted in a barely perceptible increase in leach rate.

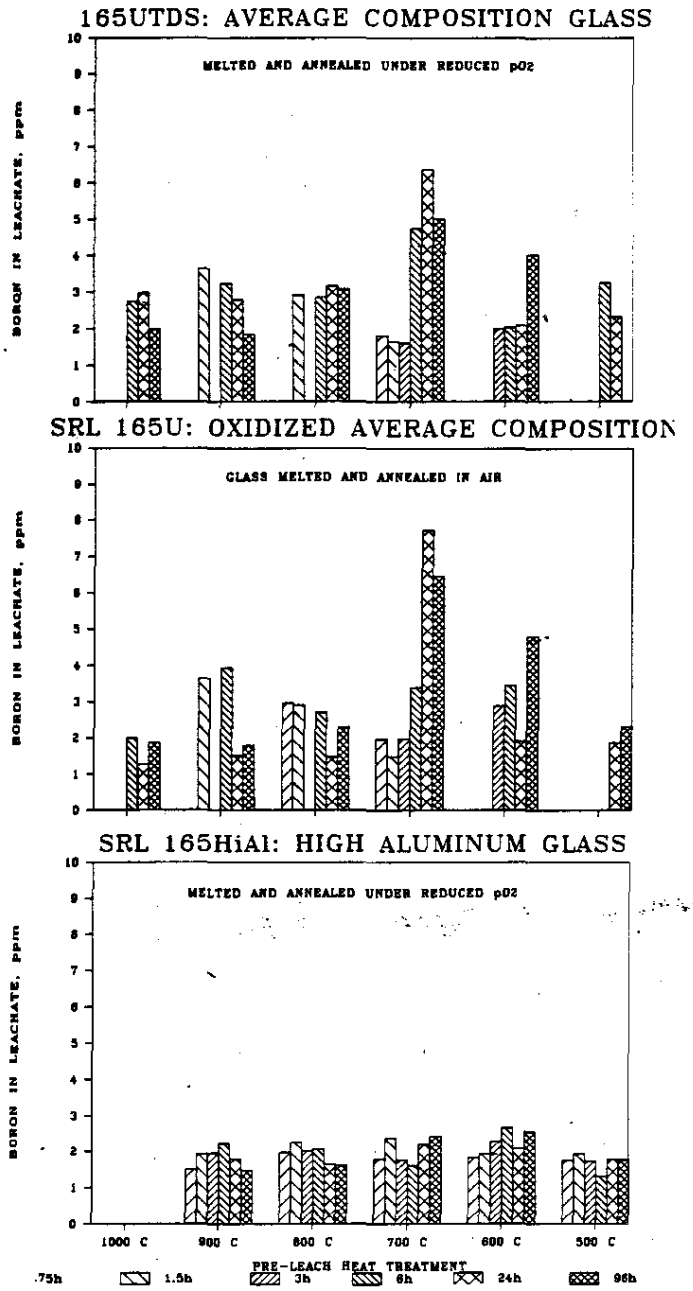

FIG. 3. Relative leach rate of devitrified SRL 165 defense waste glasses.

Comparison of leach data using the 24-hour CGW method and the 28-day MCC-1 test method [8] is given in Table II. The data for Si and B release were compared for samples in the as quenched, canister centerline cooled, and devitrified states. The leach rates were compared in units of g/m^2-day. Both tests showed that leach rates of the as quenched glasses and the glasses cooled following a simulated canister centerline cooling curve were similar while extreme devitrification increased the leach rate of Si and B by only a factor of 2 to 3 times. The MCC-1 leach test is more sensitive to small percentages of devitrification such as observed in the centerline cooled samples, but for rapid determination of the effects of devitrification, the CGW 24-hour test provides an accurate determination of leach rate enhancement.

CONCLUSIONS

The role of oxygen fugacity during glass melting is important in understanding potential crystallization during melter idling, transportation accidents, or long-term repository storage. Kinetic and equilibrium thermodynamic principles of simple melt systems have been applied to multicomponent waste-glass systems, simplifying interpretation.

TABLE II. Comparison of MCC-1 and Accelerated Leach Test Methods on 165UTDS Glass

	Leach Rate (g/m^2-d)			
	Silicon		Boron	
Condition	MCC-1	CGW*	MCC-1	CGW
Quenched	0.45	0.24	0.48	0.28
Simulated production canister centerline cooling	0.63	0.22	0.75	0.28
Heat treated 24 hours at 700°C	0.79	0.40	1.25	0.74

* CGW is a 24-hour test of powdered waste glass between 100 and 200 mesh with an effective ground SA/V of 4.3 cm^{-1}.

TTT diagrams have been completed for glass made under reducing (normal melter operation) and oxidized (melter idling) conditions for average and high aluminum SRP defense waste glasses. The glasses are homogeneous when melted at 1150°C and do not crystallize when air quenched from this temperature, or when isothermally annealed below 550°C.

Glasses made under reduced oxygen fugacity show the least volume percentage crystallization. The reduction of alkali content in SRL 165 formulations from previous formulations, e.g., SRL 411, 211, and 131 has eliminated [5] the leachable devitrification products lithium metasilicate and nepheline. As a consequence, devitrification of 30 vol % results in only a factor of about 3 increase in the leach rate, making devitrification less significant than in earlier formulations, where up to 40X increases have been reported [16]. The formation of spinel has little or no effect on leachability, while the formation of acmite produces a noticeable but small increase in the rate of dissolution of the matrix glass. This may be attributed to differences in

thermal expansion coefficients and the resulting residual stresses [11], or to the relative solubilities of oxides and silicates. No direct evidence of microcracking was observed. The lack of significant effect on leachability of devitrified radioactive waste glass [17] has been confirmed at higher than normal crystallizations. Thus, leach rates from SRL glass subjected to accident conditions, or moderate temperatures for long time periods will be similar to those of unaged glass with a similar composition.

All observed crystallization is heterogeneous, with the melt insoluble RuO_2 as the principal nucleating agent. Chromium stimulates spinel formation at 800° to 900°C. In the 650° to 800°C regime, acmite ($NaFeSi_2O_6$) is heterogeneously nucleated by RuO_2. The initial acmite is acicular and enriched in nickel. This, in turn, serves as a nucleating agent for massive acmite crystals with much lower nickel content.

Kinetics of transformation, and the composition of the devitrified phases, are influenced by oxygen fugacity. Low oxygen fugacity favors spinels that are rich in iron, and acmite low in silicon. Oxygen fugacity may also affect the solubility and dispersion of critical nucleating agents, such as RuO_2, as well as control the path of crystallization. The kinetics of devitrification follow the trends delineated for simpler glasses.

ACKNOWLEDGEMENTS

The authors wish to thank C-L. W. Hsu for scanning electron microscopy, P. E. O'Rourke for electron microprobe analyses, D. G. Karraker for magnetic susceptibility and Mossbauer spectroscopy analyses, and B. C. Osgood for assistance in x-ray diffractometry.

REFERENCES

1. G.E. Raines, L.D. Rickertsen, H.C. Claiborne, J.L. McElroy, and R.W. Lynch, Scientific Basis for Nuclear Waste Management, 3, Plenum Press, NY (1981).
2. R.P. Turcotte, and J.W. Wald, PNL-2247, Pacific Northwest Laboratory, Richland, WA (1978).
3. R.P. Turcotte, J.W. Wald, and R.P. May, Scientific Basis for Nuclear Waste Management, 2, Plenum Press, NY, 141-148 (1980).
4. P.I.K. Onorato and D.R. Uhlmann, J. Non-Crystalline Solids, 22, 367-378 (1976).
5. C.M. Jantzen, D.F. Bickford, and D.G. Karraker, Proceedings of Second International Symposium on Ceramics in Nuclear Waste Management, American Ceramics Society (1983).
6. H. D. Schreiber, et al "An Electromotive Force Series in a Borosilicate Glass-Forming Melt," submitted for publication in Science, January 1984.
7. C.M. Jantzen and D.G. Karraker, "Quantative X-ray Diffraction and Magnetic Susceptibility for Devitrification Studies," to be published in Journal of American Ceramic Society.
8. D.M. Strachan, B.O. Barnes, and R.P. Turcotte, Scientific Basis for Nuclear Waste Management, 3 Plenum Press, NY, 347-354 (1981).
9. P. G. Shewmon, Transformations in Metals, McGraw Hill, Inc., New York (1969)
10. A.A. Minaev, S.N. Oziraner, and N.P. Prokhorova, Ceramics in Nuclear Waste Management, Conf-790420, 229-232 (1979).
11. G.W. Beall and H.L. Rittler, Am. Ceram. Soc. Bull, 55, [6], 579-582 (1976).
12. K.A. Jackson, Liquid Metals and Solidification, 174, ASM, Cleveland (1958).
13. W. Guber, M. Hussain, L. Kahl, W. Muller, J. Saidl, Ceramics in Nuclear Waste Management, Conf-790420, 285-192 (1979).
14. J.T. Dalton, K.A. Boult, H.E. Chamberlain, and J.A.C. Marples, Proceedings of Intl. Seminar on Chemistry and Process Engineering for High Level Liquid Waste Solidification, Julich, W. Germany, July-Conf 42, 515-532 (1982).
15. A. Malow, Ceramics in Nuclear Waste Management, Conf-790420, 203-209 (1979).
16. L.L. Hench and D.E. Clark, NUREG/CR-3472, 347-354 Vol. 1 (1983).
17. N.E. Bibler, Glastechn. Ber, 56K, 736-742 (1983).